Kinetics of Carbonate Mineral Dissolution in CO_2-Acidified Brines at Storage Reservoir Conditions

Cheng Peng, Benaiah U. Anabaraonye, John P. Crawshaw, Geoffrey C. Maitland, and J. P. Martin Trusler*

Qatar Carbonates and Carbon Storage Research Centre, Department of Chemical Engineering, Imperial College London, South Kensington Campus, London SW7 2AZ, U.K.

* To whom correspondence should be addressed. E-mail: m.trusler@imperial.ac.uk

Abstract

We report experimental measurements of the dissolution rate of several carbonate minerals in CO_2-saturated water or brine at temperatures between 323 K and 373 K and at pressures up to 15 MPa. The dissolution kinetics of pure calcite were studied in CO_2-saturated NaCl brines with molalities of up to 5 mol·kg^{-1}. The results of these experiments were found to depend only weakly on the brine molality and to conform reasonably well with a kinetic model involving two parallel first-order reactions: one involving reactions with protons and the other involving reaction with carbonic acid. The dissolution rates of dolomite and magnesite were studied in both aqueous HCl solution and in CO_2-saturated water. For these minerals, the dissolution rates could be explained by a simpler kinetic model involving only direct reaction between protons and the mineral surface. Finally, the rates of dissolution of two carbonate-reservoir analogue minerals (Ketton limestone and North-Sea chalk) in CO_2-saturated water were found to follow the same kinetics as found for pure calcite. Vertical scanning interferometry was used to study the surface morphology of unreacted and reacted samples. The results of the present study may find application in reactive-flow simulations of CO_2-injection into carbonate-mineral saline aquifers.

Keywords: carbon storage; calcite; carbon dioxide; chalk; dissolution; dolomite; kinetics; limestone; magnesite.

1. Introduction

Deep saline aquifers are considered to be favourable sinks for the geological storage of carbon dioxide captured from power-plant and other industrial sources. The estimated capacity of such aquifers is sufficient to support carbon dioxide storage on a massive scale and much of the technology required to implement this has been developed in connection with petroleum exploration and production (1). Of course, many technical issues arise when assessing the suitability of a given aquifer as a storage sink and there are presently gaps in our knowledge that call for further research. One specific area of uncertainty relates to chemical interactions between injected CO_2 and the reservoir fluids and rocks. In particular, dissolution of carbon dioxide in the reservoir brines gives rise to an acidic solution that may react with the rocks, especially when these contain carbonate minerals, with consequent changes in the porosity and permeability of the formation (2). In order to quantify such changes, it is necessary to have a fundamental quantitative understanding of the kinetics of mineral dissolution under realistic conditions of temperature, pressure and brine salinity.

One approach to this problem is to investigate the changes in the porosity and permeability of rock cores that occur when acidified aqueous solutions displace neutral brine during a flow experiment. In such an experiment, the observed behaviour arises from a combination of advection, diffusion and reaction phenomena. Thus, in the complex geometry of the rock pore space, the results can be difficult to interpret. Accordingly, the purpose of the present research is to assess the surface reaction rates of carbonate minerals in contact with CO_2-acdified brines under reservoir conditions of temperature and pressure but free from mass-transfer limitations.

The dissolution of carbonates in CO_2-acidified media is typically represented by three parallel reactions (3):

$$\mathrm{MCO_3 + H^+ = M^{2+} + HCO_3^-} \quad (1)$$

$$\mathrm{MCO_3 + H_2CO_3 = M^{2+} + 2HCO_3^-} \quad (2)$$

$$\mathrm{MCO_3 = M^{2+} + CO_3^{2-}} \quad (3)$$

Here, M represents a bivalent cation (Ca and Mg in this study).

In a previous study of calcite dissolution kinetics in CO_2-saturated water at reservoir conditions, Peng et al (4) demonstrated that far from equilibrium surface reaction rates, r, can be described by a simple model that accounts for the contributions of reactions 1 and 2 only:

$$r = k_1 a_{\mathrm{H+}} + k_2 a_{\mathrm{CO_2}} \quad (4)$$

Here, k_1 and k_2 are the rate constants for reaction 1 and 2 respectively, and a_X denotes the activity of species X.

The impact of different brine chemistries and ionic strengths on carbonate dissolution kinetics at different conditions has been reported in literature. The bulk of these studies have been focussed on NaCl brines. Other solutes are present in both aquifer waters and seawater,

including as KCl, Na_2SO_4, $NaHCO_3$ and $CaCl_2$ among others, but NaCl typically constitutes about 90% of the dissolved salts (5). The seawater has a mean salinity (mass fraction) of around 3.5 % (5), corresponding to a NaCl molality of around 0.5 mol·kg^{-1}. However, the brines present in deep saline aquifers can have much higher salinities, ranging from around 1 mol·kg^{-1} in North Sea aquifer (6) up to as high as 5 mol·kg^{-1} in some of the aquifers of the Middle East (7, 8). There is some ambiguity in the literature regarding the specific impact of sodium chloride on the kinetics of calcite dissolution. For instance, while Finneran et al. (9) reported a decrease in calcite dissolution rates with increase in NaCl concentrations; Pokrovsky et al. (10) found the reaction rate to be independent of NaCl molality.

The dissolution kinetics of other carbonate minerals, including dolomite, magnesite and natural limestones, have been studied in the literature only at low temperature (< 323 K) with CO_2 partial pressures up to 0.1 MPa. These conditions are appropriate for seawater interactions, but not for deep saline aquifers. The first detailed experimental study on dolomite dissolution was reported by Busenberg and Plummer (11), whose study covers ranges of *p*H (1 to 10), CO_2 partial pressure (0 to 0.1 MPa) and temperature (278 to 338 K) conditions. Dolomite dissolution rates at T = 298 K were modelled with fractional reaction orders of 0.5 for reactions (1) to (3). However, this analysis was later questioned by Chou et al. (12) who measured the dissolution rates of both dolomite and magnesite using a continuous flow-through fluidized-bed reactor. They found new partial reaction orders of 0.75 for dolomite and proposed different rate-constant values at T = 298 K. Comprehensive studies of dolomite dissolution in acidic solutions were later performed by Gautelier et al. (13) using a mixed-flow reactor incorporating the rotating disc technique. Measurements were made at T = 298 K, 323 K and 353 K in the *p*H range from -0.39 to 4.44. They found that under acidic conditions, dolomite dissolution was controlled by reaction (1) alone with a reaction order that varied with temperature. Among other studies of dolomite dissolution rates, Orton and Unwin (14) used a channel flow method, while Lüttge (15) employed vertical scanning interferometry (VSI). However, there is considerable disagreement between all of these reported studies concerning both the order of the key reaction(s) and the associated rate constants.

Studies of magnesite dissolution rates are very limited. Chou et al. (12) reported magnesite dissolution rates at T = 298 K. In their work, dissolution was modelled as a first-order process dependent only on *p*H. Pokrovsky and Scott (16, 17) used a mixed-flow reactor similar to Gautelier et al. (13) to investigated magnesite dissolution kinetics at T = 298 K as a function of *p*H (from 0.2 to 12) and ionic strength (from 0.002 to 0.5 mol·kg^{-1}). Most of their experiments were conducted under far-from-equilibrium conditions and they reported a similar dependence upon *p*H under acid conditions but with rate constants that differed from those found by Chou et al. (12). Jordan and Higgins (18, 19) investigated magnesite dissolution kinetics at the microscopic scale by means of Atomic Force Microscopy and reported much smaller dissolution rates. Few experimental studies at reservoir-like conditions have been reported. However, Pokrovsky et al. (10, 20) have recently measured the dissolution of calcite, dolomite and magnesite at temperatures up to 423 K with CO_2 partial pressures up to 5.5 MPa.

In view of the relatively poor agreement between previously reported studies and the lack of adequate data at reservoir conditions, we have carried out new measurements of reaction rates of carbonate minerals in different aqueous media at reservoir conditions. These

measurements were made under conditions free from mass-transfer limitations and far from equilibrium. As previously demonstrated, studying carbonate dissolution kinetics in a CO_2-free HCl(aq) system can be very beneficial to distinguish the impacts of H^+ and dissolved CO_2 on the dissolution kinetics (4). This approach was also adopted in the current study. The present study focuses first on the effects of brine chemistry, specifically NaCl molality, on the dissolution rates of pure calcite, and second on the dissolution rates of other carbonate minerals in the CO_2-water system.

2. Methodology

2.1 Materials

In this study, we investigated the dissolution kinetics of pure calcite, pure magnesite and three natural carbonate rocks: dolomite, Ketton limestone and a North Sea chalk. The calcite samples were cleaved from a single large rhombohedral crystal of Iceland Spar obtained from Bolivia. The unreacted surface profiles of several cleavages were investigated by vertical scanning interferometry (VSI) using a Wyko NT9100 optical profiler. The surfaces appeared to be almost perfectly flat and smooth to within the resolution of the instrument, with a typical absolute average surface roughness (R_a) of about 50 nm. To test the purity of the material, small samples of the calcite were dissolved in 0.1 M HNO_3(aq) and analysed by ion chromatography (IC) with a detection limit of 50 ppb by mass. No cations other than Ca^{2+} were detected.

The single crystal magnesite sample was obtained from Brumado, Brazil. Prior to the dissolution studies, the magnesite was crushed and particles with size ranges of (100 to 150) μm and (150 to 200) μm were segregated using sieves. The specific surface area (SSA) of the segregated particles were determined by N_2 adsorption using the B.E.T. method and the SSA for (100 to 150) μm and (150 to 200) μm particles were between (0.06 to 0.075) $m^2\,g^{-1}$ and (0.04 to 0.055) $m^2\,g^{-1}$, respectively. Analysis of dissolved samples as above found no cations other than Mg^{2+}.

Each of the other materials studied was a porous mineral requiring careful preparation and surface characterisation to establish the purity and initial reactive surface area. The dolomite was cleaved from a large pink mineral sample obtained from Morocco. To test the purity of the material, five small sub-samples cleaved from different parts of the original specimen were analysed by IC and no cations other than Ca^{2+} and Mg^{2+} were found, indicating a calcium magnesium carbonate mass fraction > 99 %. Ideally, dolomite comprises pure anhydrous $CaMg(CO_3)_2$ but variations from 1:1 Ca/Mg stoichiometry are found. For the five sub-samples investigated by IC, we found that the molar ratio of calcium to magnesium was (1.15 ± 0.23). A further three sub-samples were cleaved, polished, coated with gold to a depth of 20 nm and analysed by scanning electron microscopy with energy-dispersive x-ray spectroscopy (SEM-EDX). Three points and one area were randomly selected for each sample to obtain the Ca/Mg ratio at the surface. The averaged ratio from the three samples was found to be 1.25, which is consistent with the bulk Ca/Mg ratio obtained by in the IC measurements. For the dissolution studies, small rectangular sub-samples of dolomite were cleaved, cleaned in de-ionised water

and then propan-2-ol, and impregnated with Epofix epoxy resin (Struers, Denmark) under vacuum to fill the surface porosity. Following impregnation and oven curing, the samples were ground and polished. When the finished surface was inspected by optical microscopy, epoxy-filled surface pores were easily visible on the surface and the surface porosity could be obtained by image processing. The results varied from sample-to-sample between 3 % and 9 %.

In the case of limestone and chalk, the original large samples were first cut into small rectangular chips, cleaned with de-ionised water and propan-2-ol, and dried to constant weight at a temperature of 353 K. The dehydrated samples were then impregnated with Epofix resin (Struers, Denmark) using N_2 at pressures of 8 MPa to 10 MPa as described by Shah *et al*. (21) to ensure that all the pores were filled. Epodye (Struers, Denmark), a fluorophore, was added to the epoxy to enable analysis of the surface porosity by confocal laser scanning microscopy (CLSM). The chemical purities of these samples were determined by IC and, Ca^{2+} and trace amounts of Mg^{2+} were detected. The surface porosity was measured by CLSM coupled with image segregation and analysis. The results of these pre-reaction characterisation measurements are presented in Table 1.

Table 1. Purity and porosity of dolomite and two carbonate reservoir analogues

	Dolomite	Ketton Limestone	North Sea Chalk
Purity (mass fraction)	> 99 %	98 %	99 %
Porosity from microscopy	3 % to 9 %	25 %	46 %

For the reaction experiments, prepared samples other than magnesite were embedded in discs of epoxy resin for mounting in the reactor, exposing a plane surface of between 100 mm^2 and 200 mm^2 for each experiment. The geometric surface area was determined by measuring the dimension of the exposed mineral with callipers and reactive surface area was then obtained by deducting the measured surface porosity. For calcite, surface porosity was absent; for dolomite, it was measured for each individual sample; while for the carbonate reservoir analogues, the mean surface porosity of the mineral obtained by CLSM was used. In the case of magnesite, slow dissolution kinetics required a much greater surface area and the powdered samples described above were used in a quantity of approximately 1 g.

The CO_2 was supplied by BOC with a minimum mole-fraction purity of 0.99995, deionised water with electrical resistivity > 18 MΩ·cm at T = 298 K was produced by a reverse-osmosis unit, and NaCl and $NaHCO_3$ were obtained from Sigma Aldrich with purities > 99 %. Sigma Aldrich also supplied 0.01 M HCl(aq), 0.1 M HNO_3(aq) and the reagents required for ion chromatography as detailed previously.

2.2 Batch Dissolution Experiments

Dissolution experiments were carried out in the batch-reactor system described previously (4). This system implements a variation of the rotating-disc method wherein the mineral sample is rotated rapidly in the liquid so as to reduce the mass-transfer resistance to a point at which the rate of dissolution is controlled by the surface reaction rate that we wish to measure. The

CO_2 saturated water or brine was prepared under the desired conditions of temperature and pressure in one batch reactor. meanwhile, the mineral sample was loaded in a second batch reactor, fitted with the rotating disc holder and stirrer, which was pre-charged with pure CO_2 also at the temperature and pressure under study. At the start of the experiment, the CO_2-saturated water or brine was transferred rapidly to the second batch reactor. Dissolution was monitored by withdrawing small samples of the liquor at e.g. 5 min intervals, diluting them quantitatively, and measuring the Ca^{2+} and/or Mg^{2+} concentrations. The amount of dissolved mineral at the time the sample was collected could then be calculated; plots of this quantity against time were found to be linear over the first 20 min or more of reaction, allowing the initial rate to be estimated from the slope.

For the measurements carried out in CO_2-saturated water, the Ca^{2+} and Mg^{2+} concentrations were measured by IC as described previously. Calibration was carried out with standard solutions. In the case of the measurements carried out in brine, analysis was by inductively coupled plasma mass spectrometry (ICP-MS) which is not compromised by the high salinity. Unfortunately, although ICP-MS offers much higher sensitivity than IC, the most abundant isotope of Ca, ^{40}Ca, coincides in the mass spectrum with that of the argon used in the nebuliser; measurements were therefore carried out using the ^{44}Ca peak. The low relative abundance of ^{44}Ca, about 2 %, and the low concentrations in the sample after dilution made these measurements somewhat difficult but work with standard solutions showed that a repeatability within ±10 % was achieved in practice.

3. Initial Reaction Rates for Carbonate Minerals in CO_2-Acidified Water or Brine

For each set of measurements, using the rotating disk technique, the angular velocities were increased until a regime where reaction rates were independent of transport limitation was found, as described by Peng et al. (4). For calcite, chalk and limestone, allowance was made for variation in *p*H as the mineral dissolved, according to the software PHREEQC version 3.1.4 (22), but for dolomite and magnesite *p*H changes were estimated to be negligible.

3.1 Dissolution of Pure Calcite in the (CO_2 + H_2O + NaCl) System

The (CO_2 + H_2O + NaCl) system was investigated at temperatures of 325 K to 373 K and NaCl molalities up to 5.0 mol·kg^{-1} at a constant pressure of 6.0 MPa. The experimental results are given in Table S1 of the Supplementary Data and are plotted as a function of molality in Figure 1. It can be seen that, given the experimental uncertainties, the addition of NaCl does not have a significant influence on the rate of reaction. In Figure 2, we plot the relative differences $\Delta r/r$ between these experimental dissolution rates and those calculated from the kinetic model of Peng et al. (4) defined as

$$\frac{\Delta r}{r} = \frac{r_{\mathrm{exp}} - r_{\mathrm{cal}}}{r_{\mathrm{cal}}} \qquad (5)$$

where r_{exp} and r_{cal} represent experimental and calculated reaction rates respectively. In making this comparison, the activities of H^+ and CO_2(aq) were calculated from PHREEQC. The model predicts that the addition of NaCl at m = 5.0 mol kg^{-1} and P = 6.0 MPa increases the initial dissolution rates by 30%, 21% and 14% at temperatures of 325 K, 353 K and 373 K respectively. These increases arise principally from the effect of salt on the proton activity (see

Table S2 in the Supplementary Data). Compared with the model, our data show overall a negative bias which significantly exceed the experimental uncertainty of about 15 % at high molalities of NaCl. These results are in overall agreement with the results presented by Pokrovsky et al. (10) that showed no significant changes in calcite dissolution rates with increase in sodium chloride concentrations from 0.01 M to 1.0 M whilst implementing the rotating disk technique. However, this contrasts with previous work in a *p*H-drift experiment that showed a decrease in calcite reaction rates with increase in ionic strengths at low partial pressures of CO_2 and *p*H > 5.6 (9).

The surface topologies of the calcite mineral samples were investigated by VSI both before and after reactions. Typical results are shown in Figure 3 and show a significant change from the smooth unreacted mineral to a highly-corroded surfaces after 60 minutes of reaction at two different NaCl molalities. This is consistent with our earlier work on calcite dissolution in CO_2-saturated water under similar condition of temperature and pressure (4).

3.2 Dissolution of Dolomite in the (HCl + H_2O) and (CO_2 + H_2O) Systems

The measured dissolution rate of dolomite in the (HCl + H_2O) and (CO_2 + H_2O) systems, based on both Ca^{2+} and Mg^{2+} measurements, are reported in Table S3 in the Supplementary Data. Dolomite dissolution kinetics in CO_2-free acidic solutions have also been reported in the literature (11-14, 23).

As noted in the introduction, there is disagreement in the literature regarding the reaction order with respect to H^+ for dolomite dissolution. In this study, instead of a fractional order, we propose an order of unity for reaction (1) implying that dolomite dissolves in HCl(aq) a similar manner to calcite and that the dissolution kinetics in the low *p*H regime conform to the following simple model:

$$r = k_1 a_{\mathrm{H+}} \tag{6}$$

The proton activity α_{H+} was calculated from the empirical model proposed by Peng *et al.* (24). The resulting values of $\ln k_1$, as determined from both Ca^{2+} and Mg^{2+} measurements, are plotted against $1/T$ in Figure 4 and exhibit good linear relationships and the corresponding activation energies derived from the Arrhenius equation are 19.0 ± 3.5 kJ·mol^{-1} for Ca^{2+} and 18.8 ± 2.2 kJ·mol^{-1} for Mg^{2+}. Extrapolating the model to T = 298 K, k_1 was found to be 3.4 x 10^{-5} mol·m^{-2}·s^{-1} for Ca^{2+}. This value is similar to the literature values at the same temperature: Busenberg et al. (11) reported a value of 6.5 x 10^{-5} mol·m^{-2}·s^{-1}, while Chou et al. found a value of 2.6 x 10^{-5} mol·m^{-2}·s^{-1}. Busenberg and Plummer had reported a dolomite dissolution rate of 4.0 x 10^{-5} mol·m^{-2}·s^{-1} at T = 318 K and *p*H = 3 and found the rate to be independent of the stirring rate, indicating that surface reaction controlled conditions had been achieved (25). The corresponding rate obtained from the present study interpolated to 318 K and *p*H 3 is 4.9 x 10^{-5} mol·m^{-2}·s^{-1}. Gautelier (13) reported a dissolution rate of 5 x 10^{-4} mol·m^{-2}·s^{-1} at T = 343 K and *p*H = 2.09 while, in this study, a dissolution rate of 8.5 x 10^{-4} mol·m^{-2}·s^{-1} was found at the same temperature and *p*H. However, Gautelier indicated that the reported value was obtained in a regime not free from mass-transfer limitations and, for that reason, a value lower than our is expected. Similar behaviour was also observed when comparing the values obtained in this study with data reported by Chou et al.(12) using a continuous flow-through fluidised-bed

reactor where a dissolution rate of 3.3 x 10^{-5} mol·m^{-2}·s^{-1} was reported at T = 298 K and pH = 2.75 while, in this study, the reaction rate was found to be 6.2 x 10^{-5} mol·m^{-2}·s^{-1} at the same experimental conditions.

Turning now to dolomite in the (CO_2 + H_2O) system, we find that the dissolution rates obtained from both Ca^{2+} and Mg^{2+} follow a similar trend to those observed in for calcite in the same system (4) but are smaller by a factor of around 10 at the same temperature and pressure conditions. This reduction in reactivity has been reported in other studies (26, 27). In Figure 5, we plot -log$_{10}$(r) against the calculated pH (24) for dolomite dissolution in the (CO_2 + H_2O) system at different temperatures. It can be observed that there is a satisfactory linear dependence and the slopes were found to be 1.2, 1.2, 1.0 and 1.0 at temperatures of 373 K, 353 K, 333 K, and 323 K, respectively. All are close to unity, supporting our treatment of reaction (1) as first order with rate given by equation (6). When we compare the rate constants found in the (CO_2 + H_2O) system with those in the (HCl + H_2O) system, we find them to be the same to within the experimental uncertainty of about 15 %. From this, we conclude that, unlike for calcite dissolution, reaction (2) is unimportant for dolomite under the conditions investigated in this work and that the rate is therefore described by equation (6) in both the HCl and CO_2 aqueous systems.

The dissolution rate constants k_1 so derived for both Ca^{2+} and Mg^{2+} are plotted as functions of reciprocal temperature in Figures 6(a) and 6(b). Again, a good linear relationship was observed between ln(k_1) and 1/T for both Ca^{2+} and Mg^{2+} and the corresponding activation energies derived from the Arrhenius equation were (19.1 ± 2.3) kJ·mol^{-1} for Ca^{2+} and (20.0 ± 2.6) kJ·mol^{-1} for Mg^{2+}. These values are very similar to the values of (19.0 ± 3.5) kJ·mol^{-1} for Ca^{2+} and (18.8 ± 2.2) kJ·mol^{-1} for Mg^{2+} obtained in the HCl system.

Only a few data have been reported on the rate of dolomite dissolution in CO_2-saturated aqueous systems at reservoir conditions. Recently, Pokrovsky et al. (20) reported dissolution rates in CO_2-saturated 0.1 M NaCl(aq) at temperatures up to 423 K and pressures up to 5.5 MPa. They used a rotating disc method operating at 425 rpm and reported a dissolution rate of 2.5 x 10^{-5} mol·m^{-2}·s^{-1} at T = 333 K and p = 5.0 MPa, while in the present work we find r = 6.8 x 10^{-5} mol·m^{-2}·s^{-1} at the same temperature but the slightly higher pressure of 6.0 MPa. Only a small part of this difference can be attributed to the difference in pressure, as the change in pH between 5 MPa and 6 MPa is only 0.03 according to the model of Peng et.al (24). Consequently, the most likely explanation for the difference is the elimination of mass transfer effects in the present study.

Our dolomite reaction rates can be interpolated or extrapolated by combining linear regression of the experimental ln(k_1) as a function of 1/T with Eq. 6 and we use this approach to facilitate further comparisons with the literature. Chou et al. report a reaction rate of about 1 x 10^{-5} mol·m^{-2}·s^{-1} at T = 298 K and pH = 3.5, in fair agreement with the value of 1.4 x 10^{-5} mol·m^{-2}·s^{-1} extrapolated from our date. However, Gautelier et al. found a rate of 3.2 x 10^{-5} mol·m^{-2}·s^{-1} at T = 323 K and pH = 3.11, while our value is 8.0 x 10^{-5} mol·m^{-2}·s^{-1}. The higher reaction rates obtained in this work are again consistent with the elimination of mass transfer resistance (3, 27, 28)

3.3 Dissolution of Magnesite in the (HCl + H_2O) and (CO_2 + H_2O) Systems

As with calcite and dolomite, the dissolution of magnesite was studied in both the (HCl + H_2O) and (CO_2 + H_2O) systems. The reaction rates were found to be independent of the rate of stirring and about two orders of magnitude smaller than those of dolomite under the same conditions. We conclude from this that mass transfer resistance was also negligible in our study. The experimental results are reported in Table S4 of the Supplementary Data. In figure 7(a) we plot ln(k_1) against 1/T for magnesite dissolution in (HCl + H_2O) while, in Figure 7(b) we plot the corresponding values of ln(k_1) also against 1/T. The apparent activation energy obtained from by linear regression for is (44.7 ± 7.4) kJ·mol^{-1}, which is in good agreement with the value of (41± 4) kJ·mol^{-1} reported by Higgins et al. (18). Few data exist in the literature with which to compare our results. Chou et al. (12) and Pokrovsky et al. (16) report magnesite dissolution rates at comparable *p*H values but at a temperature of 298 K only; the former are in fair agreement with the present data (extrapolated to 298 K) but the latter are about one order of magnitude smaller.

The rates of magnesite dissolution in the (CO_2 + H_2O) system were found to be in close agreement with those measured in the (HCl + H_2O) system at the same temperature and *p*H, and so that we again conclude that only reaction (1) is significant under the conditions studied in this work. In Figure (8), we plot ln(k_1) for magnesite dissolution in (CO_2 + H_2O) against 1/T and again observe a good linear correlation, from which we obtained an apparent activation energy of (43.4 ± 2.7) kJ·mol^{-1}, in close agreement with that obtain in the (HCl + H_2O) system. Furthermore, the rate constants k_1 in both the HCl and CO_2 systems are themselves in close agreement. For example, T = 353 K and 323 K, the values of ln[k_1/(m·s^{-1})] in the CO_2 system were (-13.7 and -15.2) comparing with (-13.7 and -15.1) for the HCl system. As with dolomite, these similarities in activation energy and reaction rate constants suggest that the rate of magnesite dissolution is proportional to the *p*H of the (CO_2 + H_2O) system in the temperature and pressure ranges studied in this work.

Comparing with the literature, we note that Pokrovsky et al. reported magnesite dissolution rates of 2.4 x 10^{-7} mol·m^{-2}·s^{-1} and 7.6 x 10^{-7} mol·m^{-2}·s^{-1} at p = 5.0 MPa and temperature of 323 K and 373 K, respectively; our values under the same conditions were in close agreement: 2.4 x 10^{-7} mol·m^{-2}·s^{-1} and 9.7 x 10^{-7} mol·m^{-2}·s^{-1} at 323 K and 373 K, respectively Linear regression of our values of lnk_1 as a function of 1/T, combined with Eq. 6, gives a reaction rate for magnesite dissolution in (CO_2 + H_2O) at T = 298 K and *p*H = 2.1 of 5.4 x 10^{-7} mol·m^{-2}·s^{-1}, which compares reasonably well with the value of 4 x 10^{-7} mol·m^{-2}·s^{-1} reported by Chou et al. at the same temperature and *p*H conditions.

3.4 Dissolution of Carbonate Reservoir Analogue Minerals in the (CO_2 + H_2O) System

Experiments on Ketton limestone and North-Sea Chalk were performed at 353 K and under a CO_2 pressure of 6.0 MPa by the rotating-disc method. The rotational angular velocity of the sample was maintained at 73 s^{-1} for both analogue samples in order to eliminate mass-transfer effects. It was observed that the dissolution profiles for Ketton limestone and North Sea Chalk follow the same trends as found for single calcite crystals (4). The reactive surface area of the sample was obtained by subtracting the pore area from the geometric surface area. The average dissolution rates for Ketton limestone and North-Sea chalk were 8.3 x 10^{-4} mol·m^{-2}·s^{-1}

and 7.4 x 10^{-4} mol·m^{-2}·s^{-1}, respectively. These results compared with those for pure calcite crystals (4) at the same experimental conditions (7.7 x 10^{-4} mol·m^{-2}·s^{-1}) Figure 9.

The surfaces of the unreacted and reacted minerals were studied by VSI. Figure 10 shows the results for the Ketton limestone. The unreacted material is seen to be almost as flat and smooth as the unreacted samples of cleaved calcite shown in Figure 3, while the reacted surface is highly corroded and partially reveals the grain structure of the rock.

The experimental dissolution rates for these two carbonate reservoir analogue rocks suggest that the results from studies of pure calcite can be applied directly to natural calcite-rich minerals provided that the reactive surface area is quantified.

4. Conclusion

The present work supports several conclusions. First the experimentally-determined effect of high salinity on the dissolution kinetics of pure calcite is small under reservoir conditions of temperature and pressure. Second, the dissolution rates of dolomite and magnesite are much lower than those of calcite and appear to be determined by *p*H alone. Finally, calcite-rich carbonate minerals appear to react at much the same rate as pure calcite itself. The consistency between the experimental values for the reservoir analogue samples and the calculated pure calcite data suggested that the kinetic models and the associated parameters derived from this study can be incorporated into reservoir simulators in order to provide more accurate reaction-transport simulations for future large-scale carbon storage projects.

Acknowledgement

This work was carried out as part of the activities of the Qatar Carbonates & Carbon Storage Research Centre (QCCSRC). We gratefully acknowledge the funding of QCCSRC provided jointly by Qatar Petroleum, Shell, and the Qatar Science and Technology Park, and their permission to publish this research.

References

1. Metz B, O. Davidson, H. C. de Coninck, M. Loos, and L. A. Meyer, editor. IPCC special report on carbon dioxide capture and storage. Cambridge, United Kingdom and New York, NY, USA: Cambridge University Press; 2005.
2. Yang F, Bai BJ, Tang DZ, Dunn-Norman S, Wronkiewicz D. Characteristics of CO2 sequestration in saline aquifers. Petrol Sci. 2010;7(1):83-92.
3. Plummer LN, Wigley TML, Parkhurst DL. Kinetics of Calcite Dissolution in Co2-Water Systems at 5-Degrees-C to 60-Degrees-C and 0.0 to 1.0 Atm Co2. Am J Sci. 1978;278(2):179-216.
4. Peng C, Crawshaw JP, Maitland GC, Trusler JPM. Kinetics of calcite dissolution in CO2-saturated water at temperatures between (323 and 373) K and pressures up to 13.8 MPa. Chemical Geology. 2015;403:74-85.
5. Walther JV. Essentials of geochemistry: Jones & Bartlett Publishers; 2009.
6. Bentham M, Kirby G. CO2 storage in saline aquifers. Oil Gas Sci Technol. 2005;60(3):559-67.
7. Kumar A, et al. Reservoir Simulation of CO2 Storage in Deep Saline Aquifers. Society of Petroleum Engineers. 2004(SPE/DOE fourteenth Symposium on Improved Oil Recovery).
8. Wagner W. Groundwater in the Arab Middle East: Springer; 2011.
9. Finneran DW, Morse JW. Calcite dissolution kinetics in saline waters. Chem Geol. 2009;268(1-2):137-46.
10. Pokrovsky OS, Golubev SV, Schott J. Dissolution kinetics of calcite, dolomite and magnesite at 25 degrees C and 0 to 50 atm pCO(2). Chem Geol. 2005;217(3-4):239-55.
11. Busenberg E, Plummer LN. The Kinetics of Dissolution of Dolomite in Co2-H2o Systems at 1.5-Degrees-C to 65-Degrees-C and O-Atm to 1-Atm Pco2. Am J Sci. 1982;282(1):45-78.
12. Chou L, Garrels RM, Wollast R. Comparative-Study of the Kinetics and Mechanisms of Dissolution of Carbonate Minerals. Chem Geol. 1989;78(3-4):269-82.
13. Gautelier M, Oelkers EH, Schott J. An experimental study of dolomite dissolution rates as a function of pH from -0.5 to 5 and temperature from 25 to 80 degrees C. Chem Geol. 1999;157(1-2):13-26.
14. Orton R, Unwin PR. Dolomite Dissolution Kinetics at Low Ph - a Channel-Flow Study. J Chem Soc Faraday T. 1993;89(21):3947-54.
15. Luttge A, Winkler U, Lasaga AC. Interferometric study of the dolomite dissolution: A new conceptual model for mineral dissolution. Geochim Cosmochim Ac. 2003;67(6):1099-116.
16. Pokrovsky OS, Schott J. Processes at the magnesium-bearing carbonates solution interface. II. Kinetics and mechanism of magnesite dissolution. Geochim Cosmochim Ac. 1999;63(6):881-97.
17. Pokrovsky OS, Schott J, Thomas F. Processes at the magnesium-bearing carbonates solution interface. I. A surface speciation model for magnesite. Geochim Cosmochim Ac. 1999;63(6):863-80.
18. Higgins SR, Jordan G, Eggleston CM. Dissolution kinetics of magnesite in acidic aqueous solution: A hydrothermal atomic force microscopy study assessing step kinetics and dissolution flux. Geochim Cosmochim Ac. 2002;66(18):3201-10.
19. Jordan G, Higgins SR, Eggleston CM, Knauss KG, Schmahl WW. Dissolution kinetics of magnesite in acidic aqueous solution, a hydrothermal atomic force microscopy (HAFM) study: Step orientation and kink dynamics. Geochim Cosmochim Ac. 2001;65(23):4257-66.
20. Pokrovsky OS, Golubev SV, Schott J, Castillo A. Calcite, dolomite and magnesite dissolution kinetics in aqueous solutions at acid to circumneutral pH, 25 to 150 degrees C and 1 to 55 atm pCO(2): New constraints on CO2 sequestration in sedimentary basins. Chem Geol. 2009;265(1-2):20-32.
21. Shah SM, Crawshaw JP, Boek ES. Preparation of microporous rock samples for confocal laser scanning microscopy. Petrol Geosci. 2014;20(4):369-74.

22. Appelo CAJ, Parkhurst DL, Post VEA. Equations for calculating hydrogeochemical reactions of minerals and gases such as CO2 at high pressures and temperatures. Geochim Cosmochim Ac. 2014;125:49-67.
23. Herman JS, White WB. Dissolution Kinetics of Dolomite - Effects of Lithology and Fluid-Flow Velocity. Geochim Cosmochim Ac. 1985;49(10):2017-26.
24. Peng C, Crawshaw JP, Maitland GC, Trusler JPM, Vega-Maza D. The pH of CO2-saturated water at temperatures between 308 K and 423 K at pressures up to 15 MPa. J Supercrit Fluid. 2013;82:129-37.
25. Marini L. Geological Sequestration of Carbon Dioxide: Thermodynamics, Kinetics, and Reaction Path Modeling. Netherlands: Elsevier; 2007.
26. Sjoberg EL. Fundamental Equation for Calcite Dissolution Kinetics. Geochim Cosmochim Ac. 1976;40(4):441-7.
27. Morse JW, Dekanel J, Harris K. Dissolution Kinetics of Calcium-Carbonate in Seawater .7. The Dissolution Kinetics of Synthetic Aragonite and Pteropod Tests. Am J Sci. 1979;279(5):488-502.
28. Sjoberg EL, Rickard DT. Calcite Dissolution Kinetics - Surface Speciation and the Origin of the Variable Ph-Dependence. Chem Geol. 1984;42(1-4):119-36.

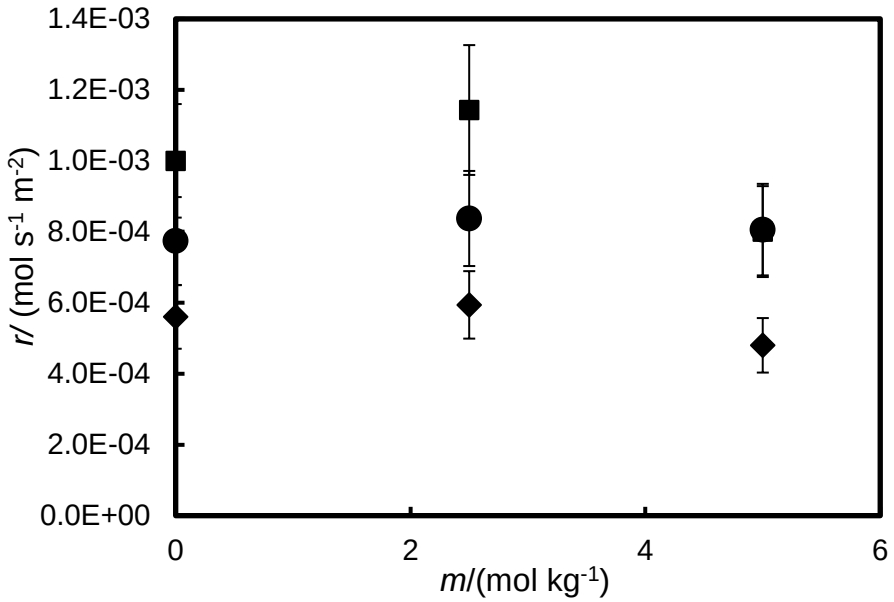

Figure 1. Dissolution rates *r* for pure calcite in (CO_2 + H_2O + NaCl) as a function of NaCl molality *m*: ■, *T* = 373 K from (4); ●, *T* = 353 K; ◆, *T* = 325 K.

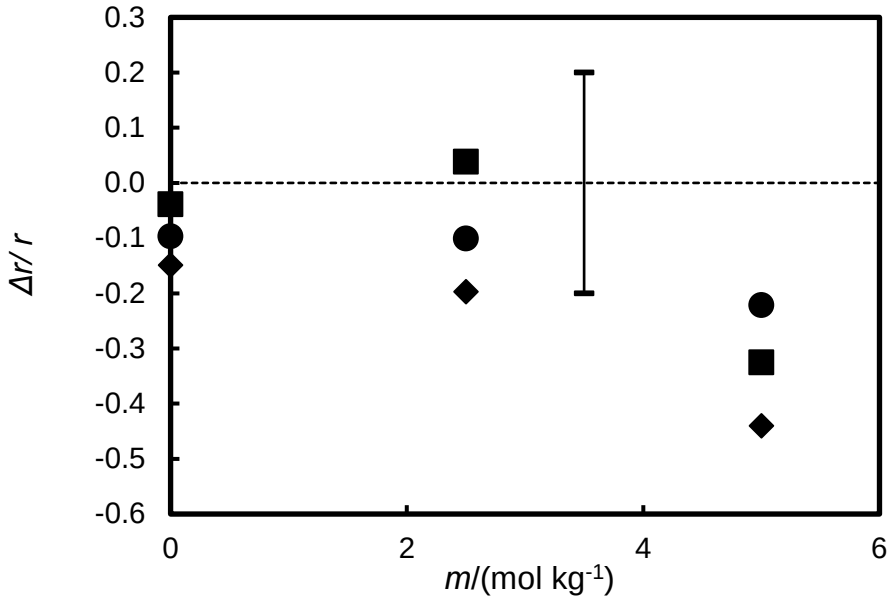

Figure 2. Relative differences Δ*r*/*r* between the experimental dissolution rates for pure calcite in (CO_2 + H_2O + NaCl) and rates calculated from equation (4) with rate constants from Peng et al. (4) and activities calculated from PHREEQC. ■, *T* = 373 K from (4); ●, *T* = 353 K; ◆, *T* = 325 K.

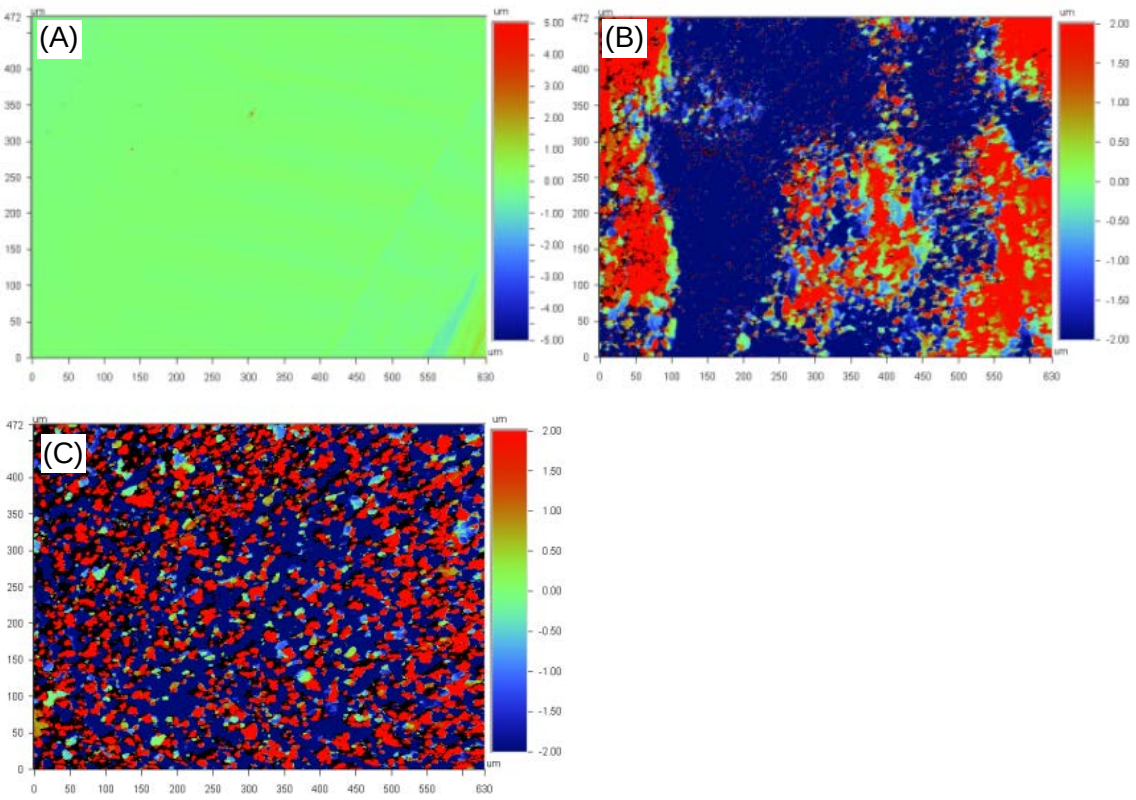

Figure 3. VSI images of calcite surfaces before and after 60 min reaction in the (CO_2 + H_2O + NaCl) system at T = 373 K and P = 6.0 MPa: (A) unreacted; (B) reacted, m = 2.5 mol kg^{-1}; (C) reacted, m = 5 mol kg^{-1}.

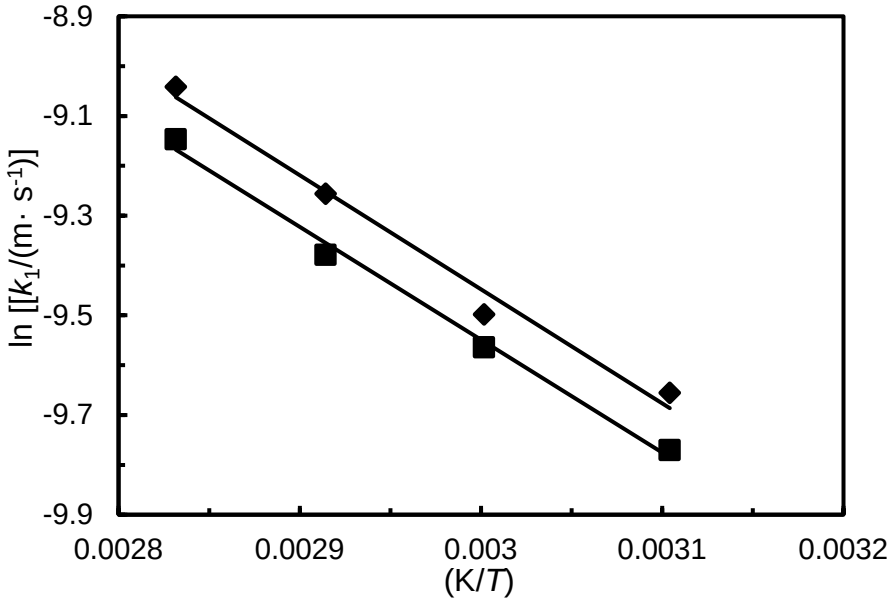

Figure 4. Natural logarithm of the rate constant k_1 for dolomite dissolution in (HCl + H_2O) as a function of inverse temperature: ◆, Ca^{2+}; ■, Mg^{2+}. Lines represent linear regressions. The experimental uncertainties are comparable to the size of the plotting symbols.

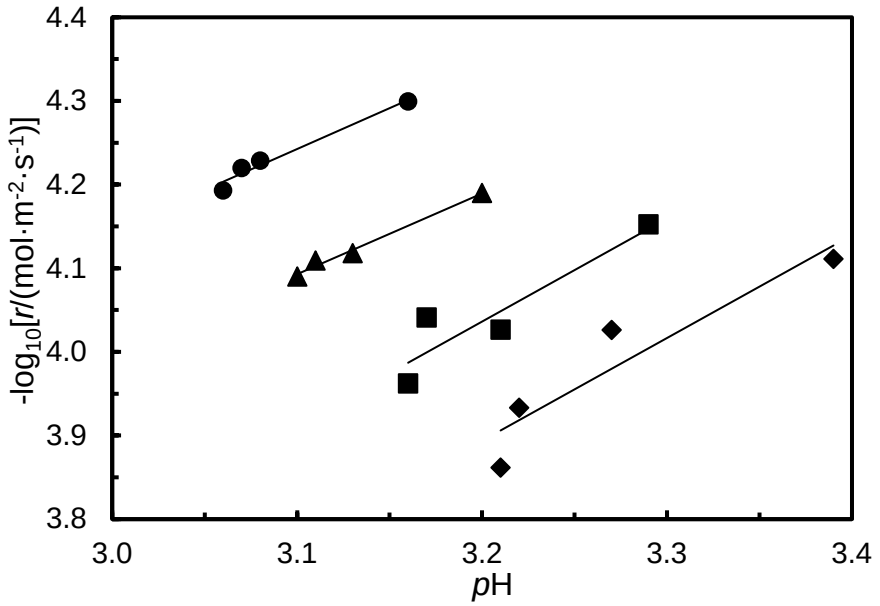

Figure 5. Relationship between $-\log_{10}(r)$, where r is reaction rate, and pH for dolomite dissolution in the (CO_2 + H_2O) system: ●, T = 323 K; ▲, T = 333 K; ■, T = 353 K; ◆, 373 K. Solid lines show linear regressions. The experimental uncertainties are comparable to the size of the plotting symbols.

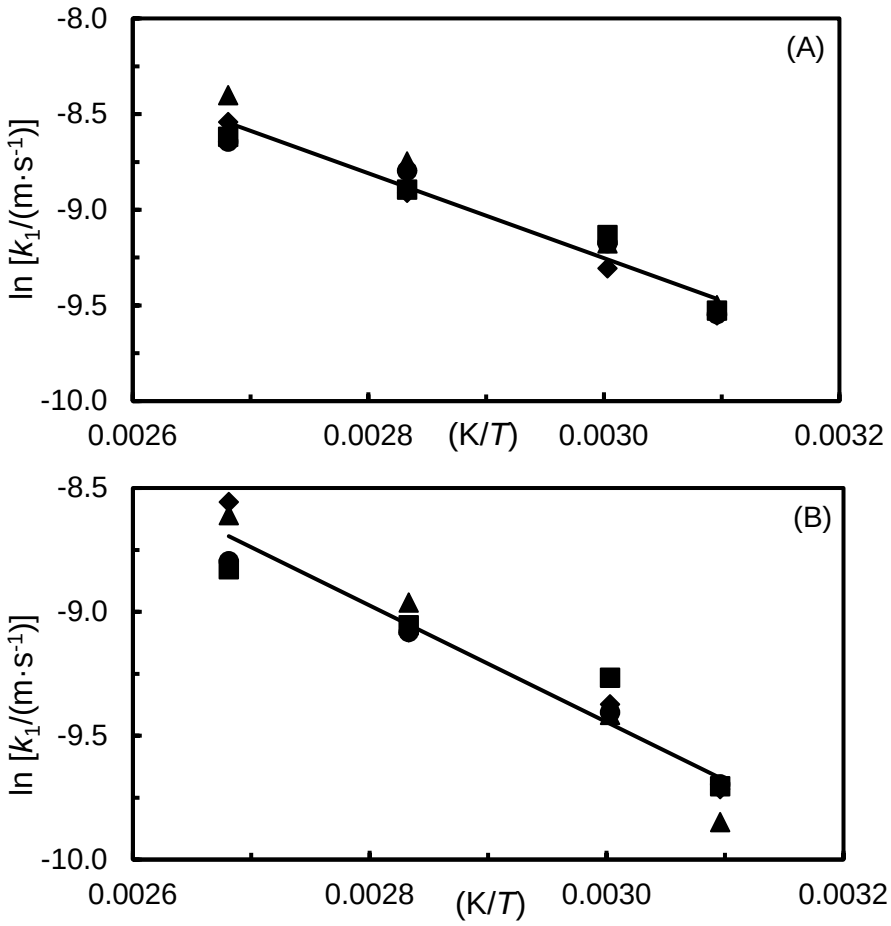

Figure 6. Natural logarithm of the rate constant k_1 for dolomite dissolution in (CO_2 + H_2O) as a function of inverse temperature at different pressures: ■, P = 6.0 MPa; ●, P = 10.0 MPa; ◆, P = 13.8 MPa; ▲, P = 15.0 MPa. (A) measurement based on Ca^{2+}, (B) measurement based on Mg^{2+}.

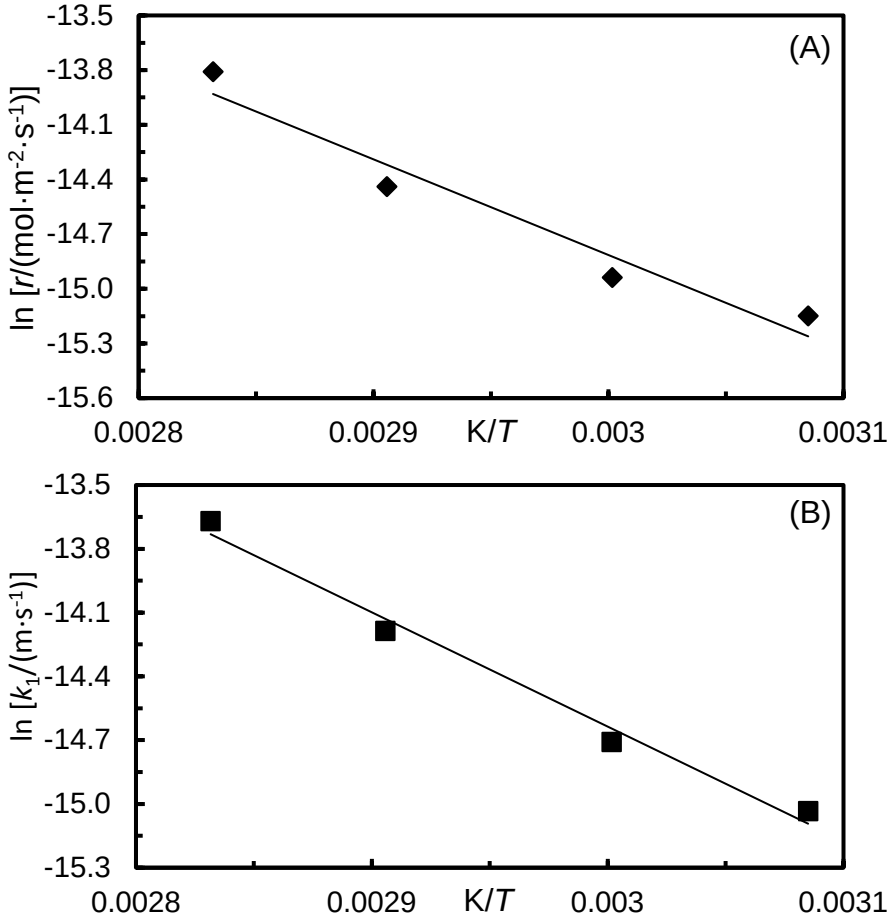

Figure 7. Natural logarithm of (A) the rate r and (B) the rate constant k_1 for magnesite dissolution in ($HCl + H_2O$) as a function of inverse temperature.

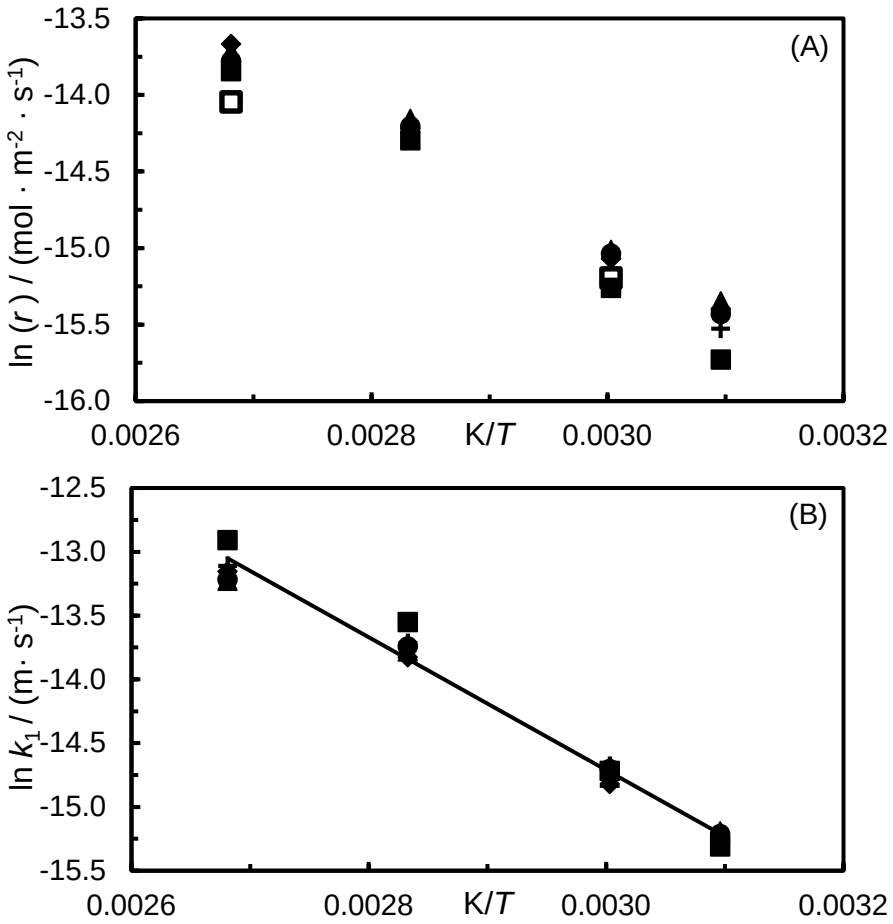

Figure 8: Natural logarithm of (A) the rate r and (B) the rate constant k_1 for magnesite dissolution in (CO_2 + H_2O) as a function of inverse temperature at different pressures:: ■, P = 5.0 MPa; +, P = 8.0 MPa; ●, P = 10.0 MPa; ◆, p = 13.8 MPa; ▲, p = 15.0 MPa. □, Pokrovsky et al. (20).

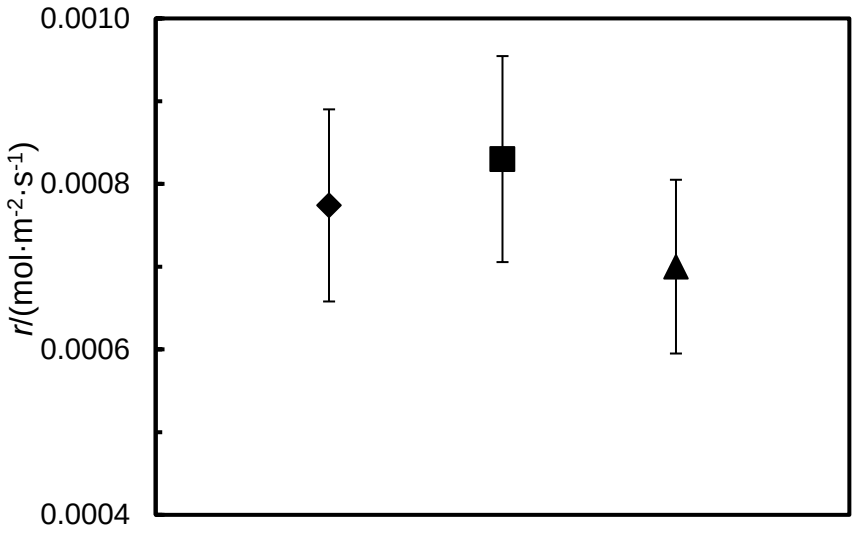

Figure 9. Comparison of the dissolution rate *r* at *T* = 353 K and *P* = 6.0 MPa: ◆, single crystal calcite; ■, Ketton limestone; ▲, North-Sea Chalk.

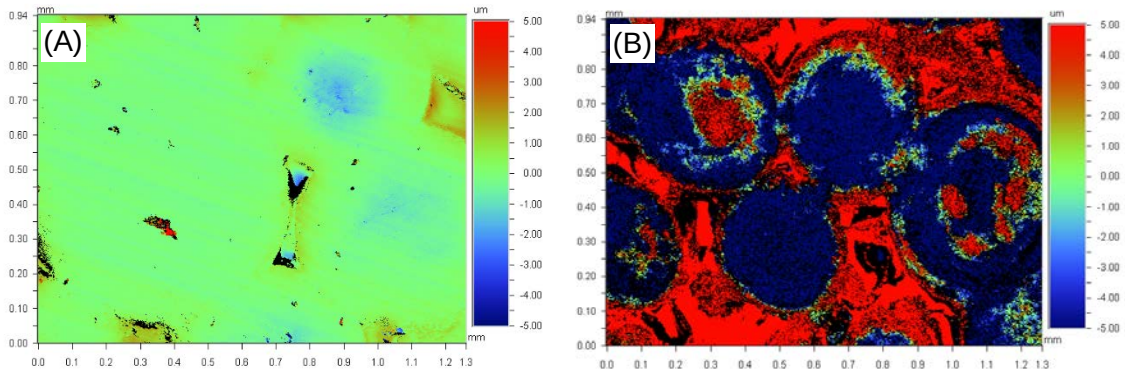

Figure 10. VSI images of Ketton limestone sample (A) before and (B) after 60 min dissolution reaction in CO_2-saturated H_2O at *T* = 353 K and *P* = 6.0 MPa.